EUROPEAN ORGANIZATION FOR NUCLEAR RESEARCH

DIFFERENTIAL AND TOTAL CROSS-SECTIONS FOR $\pi^- + p \rightarrow \eta + n$ FROM 718 TO 1050 MeV/c

W. Deinet, H. Müller, D. Schmitt and
H.-M. Staudenmaier,

Institut für Experimentelle Kernphysik,
Universität Karlsruhe and Kernforschungs-
zentrum Karlsruhe,

and

S. Buniatov*) and E. Zavattini

CERN, Geneva.

ABSTRACT

The reaction $\pi^- + p \rightarrow \eta + n$ ($\eta \rightarrow$ neutrals) has been studied by a neutron missing-mass spectrometer. Using 160 cm long neutron counters with electronic determination of the interaction point, a wide-angle range was covered. The angular distributions become clearly anisotropic at 763 MeV/c.

(Submitted to Nuclear Physics)

7 March 1969

---

*) CERN visitor, now at the Joint Institute of Nuclear Research, Dubna, USSR.

1. INTRODUCTION

At the CERN Proton Synchrotron (PS) we studied the production of the reaction $\pi^- + p \to \eta + n$ for beam momenta between 718 and 1050 MeV/c, using a neutron missing-mass spectrometer*). As the pion-nucleon scattering in this region is already considerably inelastic, the phase-shift analysis of this scattering is rendered more difficult. The results still differ on essential points. η-production data aid in clarifying the situation for the I = 1/2 resonances. The existence of the S_{11} resonance, which could not be proved unambiguously by the phase-shift analyses of the elastic πN scattering, is mainly supported by η-production data.

The measurements of Jones et al.[1] show that the η-production cross-section rises linearly from threshold up to a π^- momentum of 700 MeV/c. This indicates that η-production is mainly S-wave near threshold. Therefore one expects isotropic production near threshold. Bulos et al.[2] have measured the production angular distribution for several beam energies from threshold up to 1 GeV, and they report isotropic production distribution for the complete region. Richards et al.[3] find isotropy at 720 MeV/c, but at 785 MeV/c and higher they get large $\cos^2 \Theta$ terms in their distributions, in contradiction to Bulos et al. They also give reasons why the measurements of Bulos et al. were insensitive to anisotropy.

The measurements of Richards and Bulos were made by looking for the angular distribution of $\eta \to 2\gamma$ events in thick-plate spark chambers. In our experiment we used the missing-mass technique. We observed the neutron instead of the decay products of the η meson. The neutron scattering angle was measured, as well as the time-of-flight of the neutron. Only the decay of the "missing mass" into neutrals was accepted.

2. EXPERIMENTAL SET-UP

The set-up is shown schematically in Fig. 1. The incident pions are defined by the beam telescope $12\bar{7}$; they interact in a hydrogen

---

*) The results of these measurements can be found in greater detail in the thesis of W. Deinet (Universität Karlsruhe, 1969). Preliminary results on the angular distributions have been presented at the Heidelberg International Conference on Elementary Particles, September 1967.

target of 10 cm length and 6 cm diameter. The anticounters $\bar{3}$ and $\bar{4}$ select reactions in which only neutrals come out. The neutron is detected in one of the five scintillation counters 21 to 25, which are 160 cm long and 10 cm in diameter. Each of these scintillators is viewed at the lower end A and the upper end B by a 56 AVP phototube. The position of the neutron interaction in the scintillator is determined, with an accuracy of about ±3 cm, by comparing the arrival time of the scintillation light at the two phototubes A and B, using the usual time-to-pulse-height techniques. Also, the time differences between the arrival of the pulses in the beam reference counter 1 and in the upper and lower edges of the neutron detectors are recorded. The neutron time-of-flight is then determined with an error of about ±1 nsec by taking the average of these two measurements (apart from a constant which depends on the effective velocity of the scintillation light travelling through the neutron counter). Counters 6 were used for calibration and permanent control of the time-of-flight and the position measurement in the neutron counters; gammas coming from the target were converted by 1 mm lead plates in front of these counters. Anticounter $\bar{5}$ gives a veto if charged particles arrive in the neutron counters. Common time-to-pulse-height converters are used for the outputs of all lower and all upper phototubes, and a pattern unit indicates those phototubes that have given signals. Also, the pulse heights at the output of the phototubes at ends A and B are recorded. Events for which signals have been given by more than one phototube at end A or at end B are rejected in the analysis.

With the usual coincidence techniques, events are selected for which the neutron arrives within a preset time-of-flight interval. For each of these events, the electronic information about the neutron detection, which is contained in five scalers and one pattern unit, is recorded on paper tape. These records contain complete information about the neutron (the position measurement determines the angle Θ_n, and the time-of-flight measurements the neutron momentum p_n).

The experimental set-up also contained an array of spark chambers placed around the target for the observation of γ showers and the determination of branching ratios[4]. The spark chambers are not shown in Fig. 1 because their information is not needed for the evaluation of these data.

3. MEASUREMENTS AND DATA EVALUATION

3.1 Differential cross-sections

From the electronic information about the neutron, we derived the effective mass of the particles, produced together with the neutron, and its scattering angle Θ^* in the centre-of-mass system. Then the mass spectra for different intervals of cos Θ^* were plotted. The information on the mass is used to select η events.

For our runs at 718, 743, and 763 MeV/c, the neutron counters were placed about 4.6 metres away from the target. At 850, 890, and 1050 MeV/c, the distance was about 3 metres. Figure 2 shows as a typical example the kinematical region accepted in the run at 763 MeV/c. At this momentum, we accept in the centre-of-mass system the range $-0.7 < \cos \Theta^*_\eta < 0.9$. The mass resolution for forward-produced η is around 7 MeV fwhm. For backward-produced η, the resolution is worse and reaches 30 MeV at the end of the accepted region. There is sufficient space outside the region of the η-mass events to allow for accurate subtraction of background. This is the advantage of the long neutron counters, which cover a wide laboratory angle range. In the usual method with normal neutron counters at a fixed angle, one either moves the neutron counter to other angles or changes the beam momentum for background determination.

Accidentals and empty target rates are each about 20% of the total event rate. A test run showed that empty target events do not show a peak at the η mass. Thus no subtraction was done for these events, as this rate is subtracted with the general background subtraction. The number of accidentals depends on the angle of observation of the neutron. The last 10 nsec of our accepted region are outside the η peak. This region contains a flat background which is mainly due to $2\pi^0$ phase-space events and accidentals. Subtraction of this angular distribution in the region of the lower time-of-flight, where we observe the η, considerably reduces the non-resonant background, and above all removes the non-flat accidental contribution. After this subtraction, linear interpolation into the region under the η peak was done. The uncertainty of the background subtraction is included in the errors. The number of η events for each bin of cos Θ^* was corrected by the azimuthal acceptance of the neutron counters, the loss of neutrons by interaction in the

target and the anticounters, and the efficiency for detection of neutrons of the given energy T.

The differential cross-sections for the six momenta where we have taken data are shown in Fig. 3, and their values are given in Table 1. The distributions become more and more anisotropic with increasing beam momentum. At 718 and 743 MeV/c, the distributions can be fitted by a constant plus a small term in cos Θ^*. At 763 and 850 MeV/c, $\cos^2 \Theta^*$ terms are needed in addition. At 890 and 1050 MeV/c no fits have been done because of the small cos Θ^* range.

3.2 The influence of systematic errors on the angular distributions

The main systematic uncertainty of our data comes from the uncertainty in the energy dependence of the neutron detection efficiency.

We have measured the neutron detection efficiency at four energies[5]. We used elastic neutron-proton scattering with a continuous neutron beam of 600 MeV maximum energy. Figure 4 shows the result of the efficiency calibration, together with a smooth curve which gives the efficiency as it is used for handling the data. Statistical errors are shown. The points at 25 and 1000 MeV are derived from other measurements[6,7].

Another source of systematic error is the variation of the detection threshold along our neutron counters due to absorption of the scintillation light. By adding the pulses of the upper and of the lower phototube, the threshold variation has been reduced to ±10% over the whole 160 cm length of the scintillators. This position dependence of the threshold means a change in the efficiency of each point of the neutron counter, and it can distort the shape of the angular distributions. From the errors in measurement of the efficiency and from the uncertainty in the variation of the threshold along the neutron counter, we estimated a total uncertainty of 9% for each point. This error may also influence the shape of the angular distributions.

If one applies this extra 9% uncertainty, then for the data at 718 MeV/c one can achieve a fit with an isotropic distribution with χ^2 probability of 5%. Thus the anisotropy found at 718 MeV/c need not be significant. For 763 MeV/c and higher beam momenta the anisotropy is significant.

The angular distributions were fitted with Legendre polynomials. Table 2 shows the normalized coefficients. In order to estimate the contribution of the previously described systematic error of 9%, this error was allocated to three points of each best fit for the angular distributions. Two of these points were chosen at the ends, the third in the middle of the measurement range (Fig. 5). The position of the third point has little influence on the calculation. A new Legendre polynomial fit was done with these three points, and the resulting error was assumed to be a systematic error.

The results also appear in Table 2. The systematic error of the differential cross-sections of $\pi^- + p \rightarrow \eta + n$ ($\eta \rightarrow$ neutrals) amounts to 12%. It contains further contributions which do not influence the shape of the angular distributions.

3.3 Total cross-sections

The total cross-sections for $\pi^- + p \rightarrow \eta + n$ ($\eta \rightarrow$ neutrals) were given by the first term of the development in Legendre polynomials. These cross-sections are shown in Table 3 for the four lowest pion momenta.

4. DISCUSSION OF THE RESULTS

The total cross-sections for $\pi^- + p \rightarrow \eta + n$ ($\eta \rightarrow$ neutrals) are shown in Fig. 6. Data of other authors were added, assuming that 56% of the neutral decays of the η meson occur in two gammas[8]. Our total cross-sections join on very well to the measurements of Jones et al.[1], and also agree with those of Bulos et al.[2] and Richards et al.[3].

The angular distributions of the η production can be compared with those of Bulos et al.[2] and Richards et al.[3], who have measured over the whole range of $\cos \Theta^*$. The differential cross-sections given here are compatible with those of Richards et al. The angular distribution of our best fit at 718 MeV/c is slightly anisotropic. Richards finds isotropy in his best fit at 720 MeV/c. Due to his big statistical errors at this beam momentum, the data of Richards et al. also fit our favoured distribution. The isotropic angular distributions of Bulos et al., up to momenta of 1100 MeV/c, are not compatible with our measurements.

Apart from their total cross-section, Jones et al.[1] give also the ratio $(d\sigma/d\Omega)_{0^\circ}/(d\sigma/d\Omega)_{180^\circ}$ for pion momenta of 696, 702, 713 and 718 MeV/c, which are all compatible with zero forward-backward asymmetry. His 180° point is outside our range at 718 MeV/c; his 0° differential cross-section is within errors consistent with our value. Differential cross-ections for a very limited range of backward angles were measured by Hyman et al.[9]. Their points at 720 and 745 MeV/c join on well to our best fit at 718 and 743 MeV/c. Recent measurements of Litchfield[10] on $\pi^+ n$ interactions in a deuterium bubble chamber also agree, within their statistics, with our measurements.

The possible anisotropy of the angular distribution of 718 MeV/c indicates that at this momentum there are, in addition to the S-wave, also higher waves that contribute to the η production. The linear term at this momentum is most easily explained by an interference between the S_{11}- and P_{11}-wave. The D_{13}-wave may be responsible for the appearance of the term with $P_2(\cos\Theta^*)$ at higher energies.

Acknowledgements

We would like to thank Professor A. Citron for his helpful discussions and critical comments and, together with Professors W. Paul, P. Preiswerk and H. Schopper, for continuous support and interest. Dr. A. Menzione contributed greatly during the early stage of the experiment. It is a pleasure to thank our technicians, K. Ratz, G. Sicher and B. Smith, for their skilful technical assistance. We are indebted to the CERN Proton Synchrotron crew and technical staff for their competent assistance during the whole experiment. The participants from Karlsruhe would like to thank the Bundesministerium für wissenschaftliche Forschung for its financial support.

Table 1

Differential cross-sections for $\pi^- + p \rightarrow \eta + n$ ($\eta \rightarrow$ neutrals)

Momentum (MeV/c)	$< \cos \Theta^* \eta >$	$d\sigma/d\Omega$ (μb/sr)	Statistical error (μb/sr)	Momentum (MeV/c)	$< \cos \Theta^* \eta >$	$d\sigma/d\Omega$ (μb/sr)	Statistical error (μb/sr)
	-0.55	114	10		-0.55	151	19
	-0.45	93	12		-0.45	105	20
	-0.35	106	15		-0.35	122	21
	-0.25	108	7		-0.25	121	26
	-0.15	97	7		-0.15	118	24
718	-0.05	114	8	743	-0.05	156	24
	0.05	116	8		0.05	186	22
	0.15	118	8		0.15	160	21
	0.25	120	8		0.25	149	20
	0.35	128	8		0.35	139	20
	0.45	139	8		0.45	184	23
	0.55	122	8		0.55	161	22
	0.65	145	9		0.65	175	23
	0.75	137	10		0.75	167	23
	0.85	134	8		0.85	196	24
	-0.65	143	13		-0.55	146	23
	-0.55	124	13		-0.45	105	26
	-0.45	105	12		-0.35	70	28
	-0.35	132	12		-0.25	50	35
	-0.25	130	12		-0.15	102	22
	-0.15	121	11		-0.05	70	25
763	-0.05	135	13	850	0.05	119	25
	0.05	121	12		0.15	126	26
	0.15	124	12		0.25	113	26
	0.25	138	13		0.35	149	27
	0.35	134	13		0.45	159	31
	0.45	112	14		0.55	117	28
	0.55	154	14		0.65	164	30
	0.65	188	16		0.75	165	34
	0.75	174	16		0.85	231	36
	0.85	196	17				
	-0.35	41	16		0.05	34	17
	-0.25	18	13		0.15	53	15
	-0.15	23	17		0.25	55	14
890	-0.05	34	17	1050	0.35	82	15
	0.05	65	18		0.45	115	15
	0.15	77	20		0.55	109	15
	0.25	78	20		0.65	75	16
	0.35	113	22		0.75	79	17
	0.45	84	21		0.85	109	19
	0.55	99	20				
	0.65	132	24				
	0.75	126	26				
	0.85	130	30				

There should be added to the statistical errors, a systematic error that is composed of a normalization error of 7% and a 9% error which can change the angular distribution.

Table 2

Normalized angular distribution coefficients

Momentum (MeV/c)	First Order	Second order	Systematic error
718	A(0) = 1 A(1) = 0.26±0.06	A(0) = 1 A(1) = 0.24±0.07 A(2) = 0.04±0.09	 0.10 0.09
743	A(0) = 1 A(1) = 0.28±0.10	A(0) = 1 A(1) = 0.26±0.11 A(2) = 0.04±0.16	 0.10 0.09
763		A(0) = 1 A(1) = 0.15±0.07 A(2) = 0.32±0.09	 0.10 0.09
850		A(0) = 1 A(1) = 0.21±0.16 A(2) = 0.59±0.22	 0.10 0.10

Table 3

Total cross-sections for $\pi^- + p \rightarrow \eta + n(\eta \rightarrow \text{neutrals})$

Momentum (MeV/c)	σ (mb)	$\Delta\sigma$ (mb)
718	1.45	0.18
743	1.84	0.23
763	1.83	0.23
850	1.75	0.25

REFERENCES

1) W.G. Jones, D.M. Binnie, A. Duane, J.P. Horsey, D.C. Mason, J.A. Newth, I.K. Rahmen, J. Walters, N. Horwitz and P. Palit, Phys. Letters 23, 597 (1966).

2) F. Bulos, R.E. Lanou, A.E. Pifer, A.M. Shapiro, M. Widgoff, R. Panvini, A.E. Brenner, C.A. Bordner, M.E. Law, E.E. Ronat, K. Strauch, J.J. Szymanski, P. Bastien, B.B. Brabson, Y. Eisenberg, B.T. Feld, V.K. Fischer, I.A. Pless, L. Rosenson, R.K. Yamamoto, G. Calvelli, L. Guerriero, G.A. Salandin, A. Tomasin, L. Ventura, C. Voci and F. Waldner, Phys.Rev. Letters 13, 486 (1964).

3) W.B. Richards, C.B. Chiu, R.D. Eandi, A.C. Helmholz, R.W. Kenney, B.J. Moyer, J.A. Poirier, R.J. Cence, V.Z. Peterson, N.K. Sehgal and V.J. Stenger, Phys.Rev. Letters 16, 1221 (1966).

4) S. Buniatov, E. Zavattini, W. Deinet, H. Müller, D. Schmitt, H.-M. Staudenmaier, Phys. Letters 25 B, 560 (1967).

5) H. Müller, W. Deinet, D. Schmitt and H.-M. Staudenmaier, A neutron counter with position determination, Interner Bericht des Instituts für Experimentelle Kernphysik der Universität und des Kernforschungszentrums Karlsruhe.

6) G. Gatti, P. Hillman, W.C. Middelkoop, T. Yamagata and E. Zavattini, Nuclear Instrum. Methods 29, 77 (1964).

7) Yu. V. Galaktinov, L.G. Landsberg and V.A. Lyubimov, Nuclear Instrum. Methods 39, 351 (1966).

8) N. Barash-Schmidt, A. Barbaro-Galtieri, L.R. Price, A.H. Rosenfeld, P. Söding and C.G. Wohl, Review of Particle Properties, UCRL - 8030 Pt. I, August 1968.

9) E. Hyman, W. Lee, J. Peoples and J. Schiff, Phys. Rev. 165, 1437.

10) P.J. Litchfield, Rutherford Laboratory RPP/H/52.

Figure captions

Fig. 1 : Diagram of the set-up.

Fig. 2 : Kinematics for η production at 763 MeV/c. Abscissa: neutron time-of-flight. Ordinate: Interaction point of the neutron in the counter (0 cm corresponds to $\Theta_n \approx 10°$, and 160 cm to $\Theta_n \approx 29°$). Full lines: $\cos \Theta_{c.m.s.}$ for neutral missing mass system.

Fig. 3 : Production angular distribution of the η meson in $\pi^- + p \rightarrow \eta + n(\eta \rightarrow \text{neutrals})$. A systematic error of 9% at each point of measurement can influence the shape of the angular distributions.

Fig. 4 : Efficiency of the neutron counters for homogeneous flux of neutrons. The measured points are approximated by efficiency = 6.84 + 7.7 × exp (-0.0104 × energy in MeV).

Fig. 5 : Procedure for estimation of the systematic error of the Legendre polynomial development. A 9% systematic error was allocated to three points of the angular distribution best fit. These points were fitted with Legendre polynomials, and the resulting error of the coefficients is called the systematic error.

Fig. 6 : Total cross-sections for $\pi^- + p \rightarrow \eta + n(\eta \rightarrow \text{neutrals})$. For comparison with the measurements of Bulos et al. and Richards et al., it is assumed that 56% of the neutral decays of the η meson occur in two gammas.

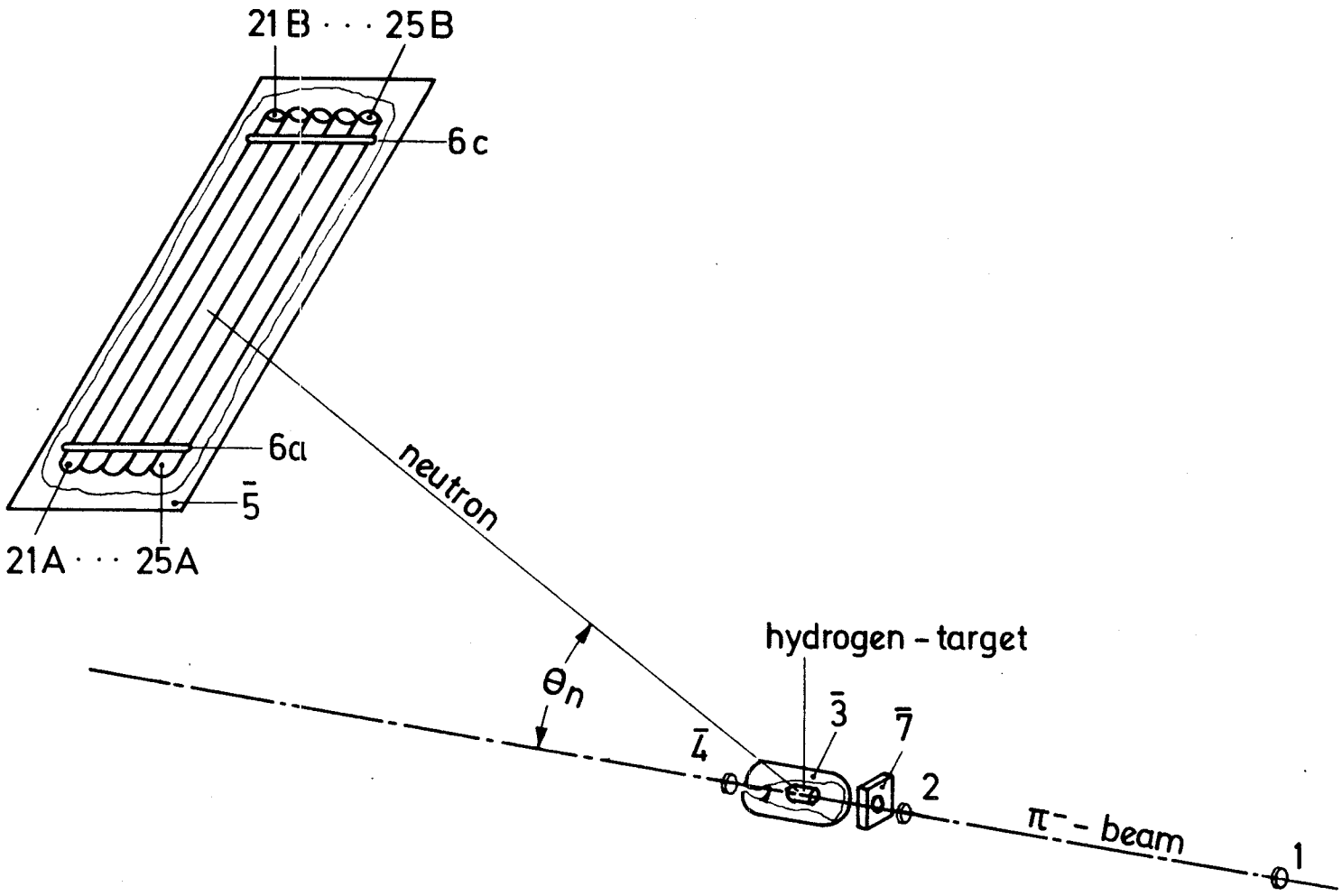
21B · · · 25B
6c
6a
5̄
21A · · · 25A
neutron
θ_n
hydrogen - target
3̄
7̄
4̄
2
π⁻ - beam
1

Fig. 1

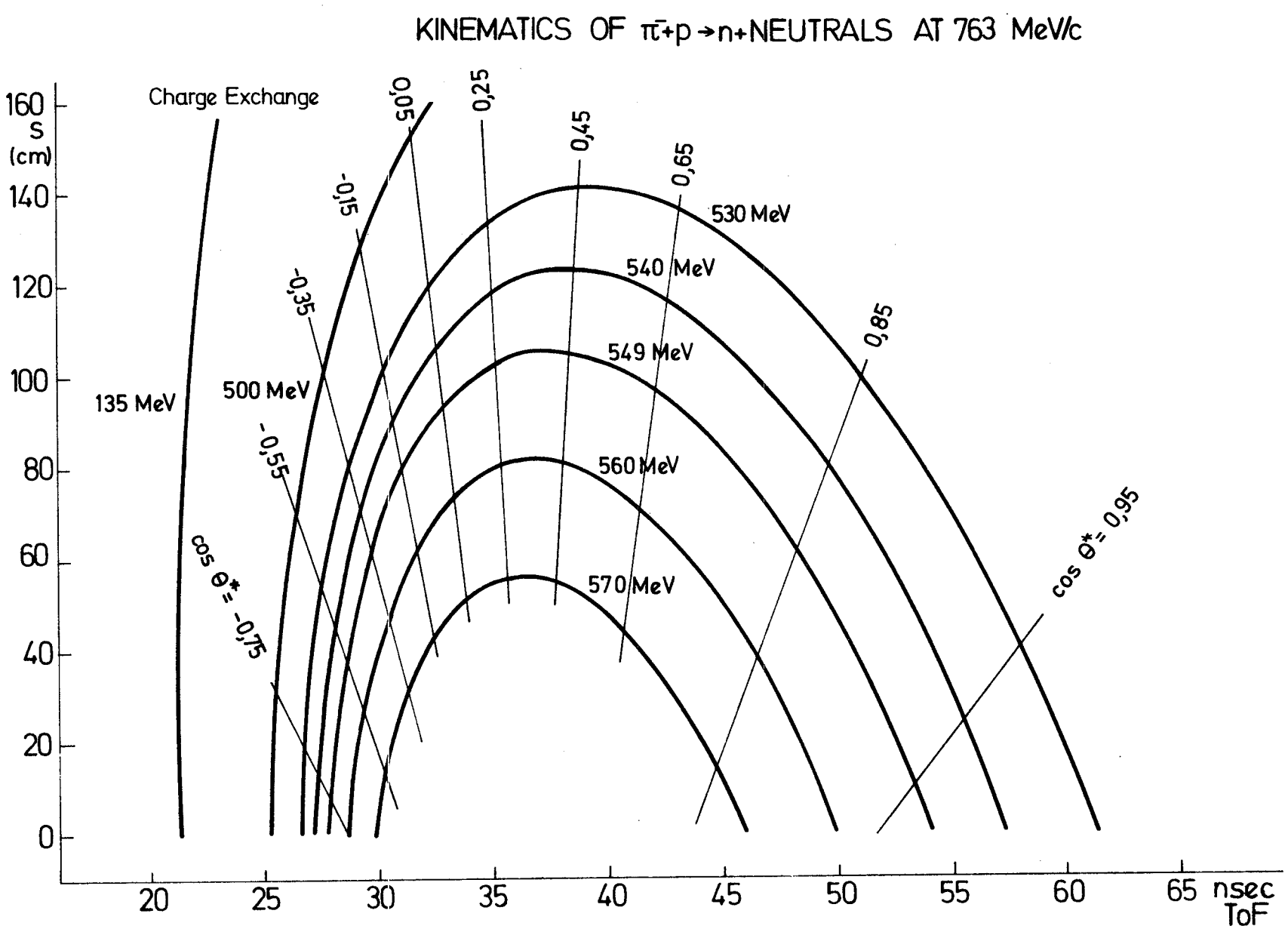
KINEMATICS OF π⁻+p→n+NEUTRALS AT 763 MeV/c
Charge Exchange
160
S
(cm)
140
120
100
80
60
40
20
0
135 MeV
500 MeV
530 MeV
540 MeV
549 MeV
560 MeV
570 MeV
cos θ*= -0,75
-0,55
-0,35
-0,15
0,05
0,25
0,45
0,65
0,85
cos θ*= 0,95
20
25
30
35
40
45
50
55
60
65 nsec
ToF

Fig. 2

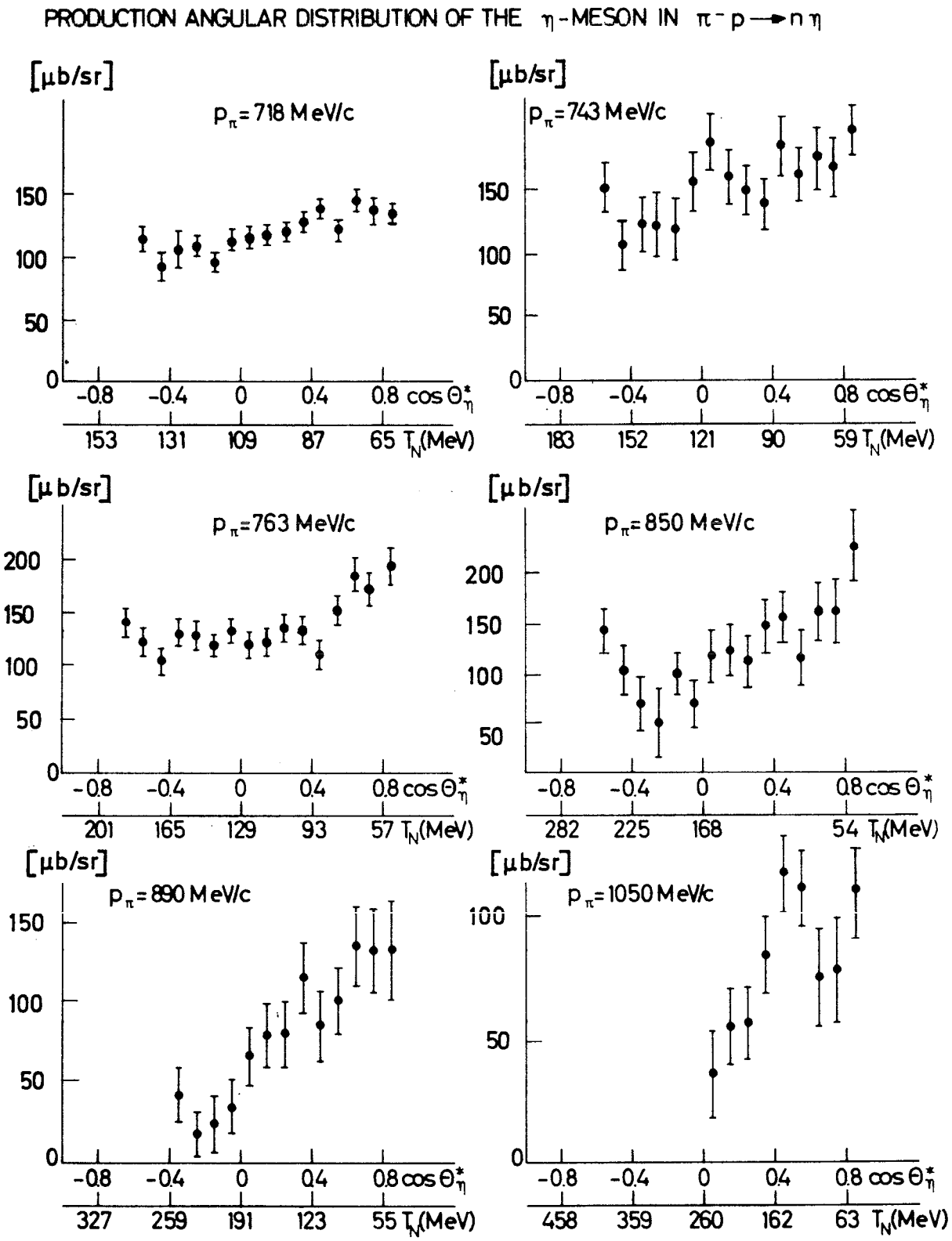
PRODUCTION ANGULAR DISTRIBUTION OF THE η-MESON IN π⁻p → nη
[μb/sr]
p_π = 718 MeV/c
150
100
50
0
-0.8 -0.4 0 0.4 0.8 cos Θ*_η
153 131 109 87 65 T_N(MeV)
[μb/sr]
p_π = 743 MeV/c
150
100
50
0
-0.8 -0.4 0 0.4 0.8 cos Θ*_η
183 152 121 90 59 T_N(MeV)
[μb/sr]
p_π = 763 MeV/c
200
150
100
50
0
-0.8 -0.4 0 0.4 0.8 cos Θ*_η
201 165 129 93 57 T_N(MeV)
[μb/sr]
p_π = 850 MeV/c
200
150
100
50
-0.8 -0.4 0 0.4 0.8 cos Θ*_η
282 225 168 54 T_N(MeV)
[μb/sr]
p_π = 890 MeV/c
150
100
50
0
-0.8 -0.4 0 0.4 0.8 cos Θ*_η
327 259 191 123 55 T_N(MeV)
[μb/sr]
p_π = 1050 MeV/c
100
50
0
-0.8 -0.4 0 0.4 0.8 cos Θ*_η
458 359 260 162 63 T_N(MeV)

Fig. 3

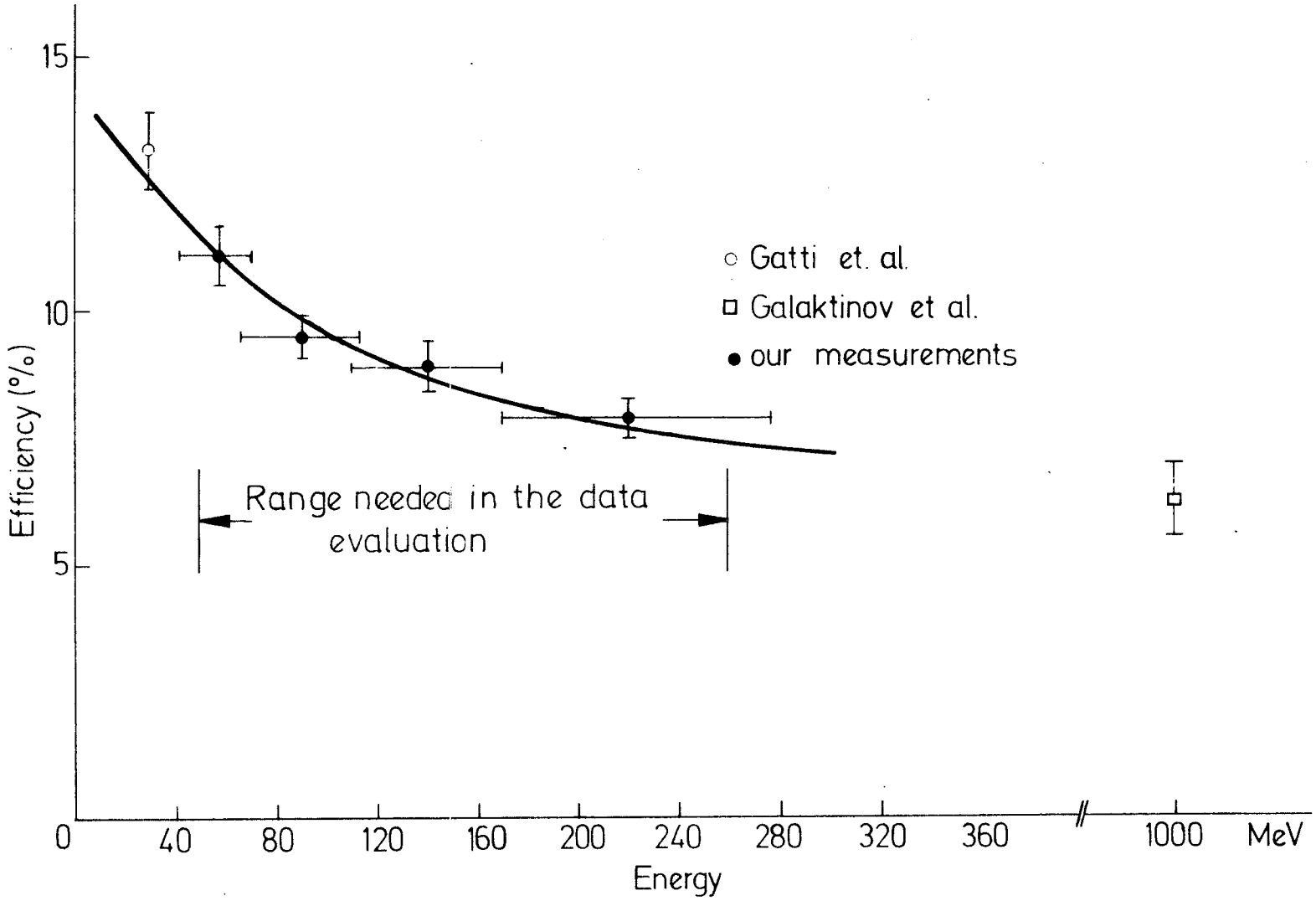
15
10
5
0
Efficiency (%)
40
80
120
160
200
240
280
320
360
1000
MeV
Energy
○ Gatti et. al.
□ Galaktinov et al.
● our measurements
Range needed in the data evaluation

Fig. 4

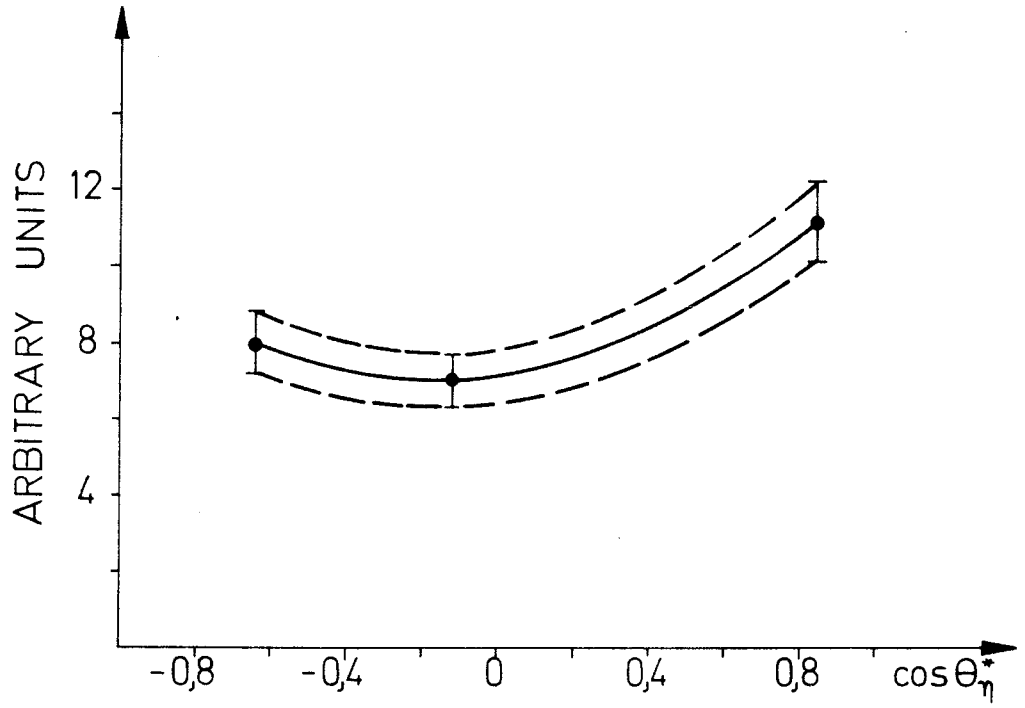

Fig. 5

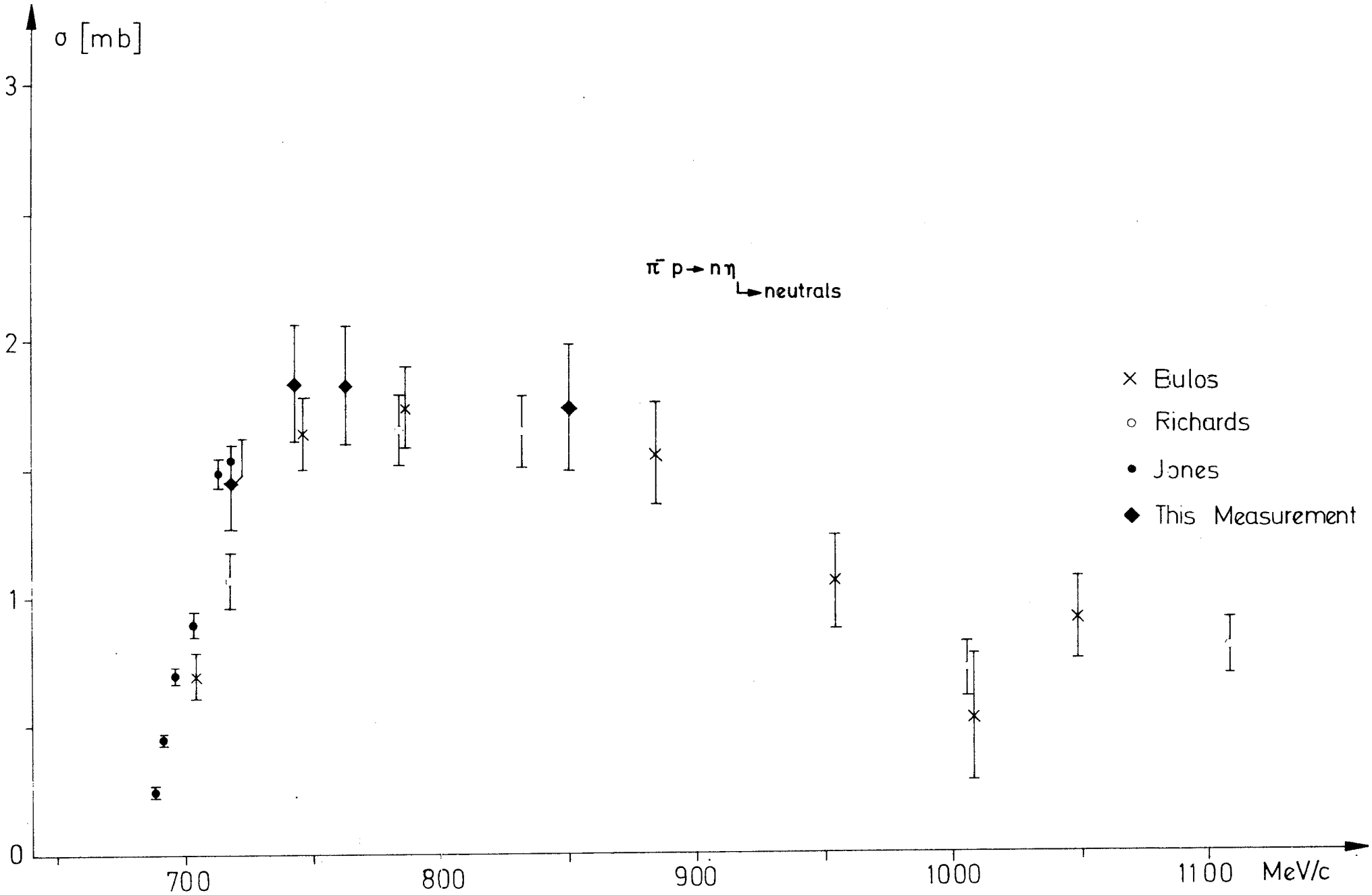
σ [mb]
3
2
1
0
700
800
900
1000
1100
MeV/c
π⁻ p → n η
↳ neutrals
× Eulos
○ Richards
• Jones
◆ This Measurement

Fig.6